Coral Reefs (2008) 27:905–911
DOI 10.1007/s00338-008-0414-3

NOTE

Electron backscatter diffraction (EBSD) as a tool for detection of coral diagenesis

M. Cusack · J. England · P. Dalbeck · A. W. Tudhope · A. E. Fallick · N. Allison

Received: 10 April 2008 / Accepted: 30 July 2008 / Published online: 15 August 2008

Abstract Fine-scale structures of intact modern and fossil coralline skeletons were analysed to determine alteration to secondary cements and phases using electron backscatter diffraction (EBSD). EBSD analysis revealed secondary aragonite cements in endolithic borings in the modern skeleton and whole dissepiments of the fossil skeleton replaced by calcite, despite X-ray diffraction (XRD) bulk analysis of the general area suggesting only aragonite was present. Non-destructive, in situ screening of coral samples by EBSD analysis provides a valuable tool for assessing the extent of alteration and can determine which areas may produce more reliable climate proxy data.

Keywords Electron backscatter diffraction (EBSD) · Diagenesis · Calcite · Dissepiments

Communicated by Geology Editor Dr. Bernhard Riegl

M. Cusack (✉) · J. England · P. Dalbeck
Department of Geographical & Earth Sciences, University of Glasgow, Gregory Building, Lilybank Gardens, Glasgow G12 8QQ, UK
e-mail: Maggie.Cusack@ges.gla.ac.uk

A. W. Tudhope
School of Geosciences, Grant Institute, University of Edinburgh, Edinburgh EH9 3JW, UK

A. E. Fallick
Scottish Universities Environmental Research Centre, Rankine Avenue, East Kilbride G75 0QF, UK

N. Allison
School of Geography & Geosciences, University of St. Andrews, St. Andrews KY16 9AL, UK

Introduction

The value of annually banded reef-building corals as recorders of climate information is well established (Gagan et al. 2000; Cole 2003; Felis and Pätzold 2003; Correge 2006; Grottoli and Eakin 2007). In particular, the stable oxygen isotope composition of coral aragonite has proven to be a powerful tool for reconstructing past sea surface temperature (SST) and sea water $\delta^{18}O$, which is closely related to salinity conditions, while the trace element composition of coral aragonite can yield records of past SST. These records can have monthly or even finer scale temporal resolution over several centuries, as a consequence of the maximum life span of an individual colony, with dead (fossil) corals providing evidence for climate change in the late Quaternary. Such coral-derived records have provided important evidence for the nature, drivers and global implications of tropical climate variability and change, including improved understanding of major features of the global climate system, such as the El Niño Southern Oscillation and the monsoon systems (Tudhope et al. 1996, 2001; Evans et al. 1998; Urban et al. 2000; Charles et al. 2003; Cobb et al. 2003) and whole tropical temperatures (Wilson et al. 2006). Recent studies of North Atlantic Oscillation and mid-latitude climate variability have been obtained from annually banded corals from subtropical oceans (Cohen et al. 2004; Kuhnert et al. 2005). *Porites* is reported to display no species-specific effects on proxy data (Maier et al. 2004); thus, *Porites* is well suited to analysis for environmental proxies such as $\delta^{18}O$ and Sr/Ca ratios.

Despite this, many small-scale variations have been described in coral skeletons with the biology of the system exerting a vital effect on the chemical signature of the coral (Cohen et al. 2002; Cohen and McConnaughey 2003; Meibom et al. 2003, 2004, 2006, 2007; Mitsuguchi et al.

2003; Allison and Finch 2004; Allison et al. 2005; Gabitov et al. 2006; Gaetani and Cohen 2006a, b). In addition to considering vital effects, it is necessary to avoid samples that are diagenetically altered (Guilderson et al. 1994, 2001; Tudhope et al. 1995, 2001; Woodroffe and Gagan 2000; Muller et al. 2001; Allison et al. 2007; Hendy et al. 2007). Until recently, coral samples were assessed using X-ray diffraction (XRD) to determine the extent of diagenetic alteration to calcite (Guilderson et al. 1994; Esat et al. 1999; Hughen et al. 1999). However, the relatively low sensitivity of XRD means that trace material (~1–2%) is not always detected (Jenkins and Snyder 1996), and this fraction can have a significant effect on climate proxies, as observed in screening through secondary ion mass spectrometry (SIMS) (Allison et al. 2007) and Raman spectroscopy (Nothdurft et al. 2007). Stable isotope and trace element climate proxies are often measured on a spatial scale of micrometres to nanometres using techniques such as SIMS, laser ablation inductively coupled plasma mass spectrometry (LA-ICP-MS) and electron probe microanalysis (EPMA). A diagenetic screening technique that operates at similar spatial resolution is therefore desirable. Electron backscatter diffraction (EBSD) has recently emerged as a significant tool in the field of materials science (Wright and Adams 1991, 1992; Adams et al. 1993, Wright et al. 1994; Schwartz 2000). Following early work by Nishikawa and Kikuchi (1928a, b) on diffraction patterns of electrons from crystalline sample surfaces, the development of an automated in situ non-destructive analysis technique that determines crystallographic information from materials has been gradually developed during the last century (Alam et al. 1954; Venables and Harland 1973; Dingley 1981, 1984; Dingley and Razavizadeh 1981; Schwarzer 1997a, b). However, EBSD application in biominerals has only recently been undertaken (Schmahl et al. 2004; Cartwright and Checa 2006; Dalbeck et al. 2006; Dalbeck and Cusack 2006; Cusack et al. 2007, 2008; England et al. 2007; Perez-Huerta et al. 2007), which has allowed in situ phase identification and crystallographic information to be obtained from these biogenic systems in a field of view of nanometres to hundreds of microns. Here, EBSD was applied to *Porites* corals to assess this technique as a means of detecting small amounts of diagenetic alteration at fine spatial resolution appropriate for climate proxy measurements made via techniques, such as SIMS, LA-ICP-MS and EPMA.

Materials and methods

A core from a living specimen of massive *Porites* sp. (cf. *lutea*) coral was obtained from Jarvis Island 0°22.3′ S, 159°59.0′ W and a fossil specimen was cored from a raised reef in the Huon Peninsula (Chappell 1974) in Papua New Guinea. Previous studies on cores from these specimens have detailed the environmental (Marriott et al. 2004) and geological settings of these specimens and the extent of diagenesis in the fossil sample (Tudhope et al. 2001).

XRD analysis was performed on a Phillips PW 1050/35 with vertical goniometer along with a Co Kα Fe-filtered radiation tube. The scanning speed was 2°2θ/min and the resultant profiles were compared with the Joint Committee on Powder Diffraction Standards (JCPDS) database.

Sections of the coral cores were reduced to ~2–3 cm and mounted in Araldite resin. The resin blocks were mounted on thin-glass section slides and the samples were polished through a series of grinding and polishing discs. The sample surface was ground down using diamond impregnated papers at 74 μm and then 20 μm, diamond slurry at 8 and 6 μm followed by a compound diamond pad at 6 and 3 μm. Polishing stages were performed with alpha aluminium oxide at 1 and 0.3 μm and the final treatment with 0.06 μm colloidal silica on a short nap disc to ensure removal of any residual damaged surface layers with local stress and deformity produced during the harder compound grinding and polishing (Prior et al. 1999; Nowell et al.

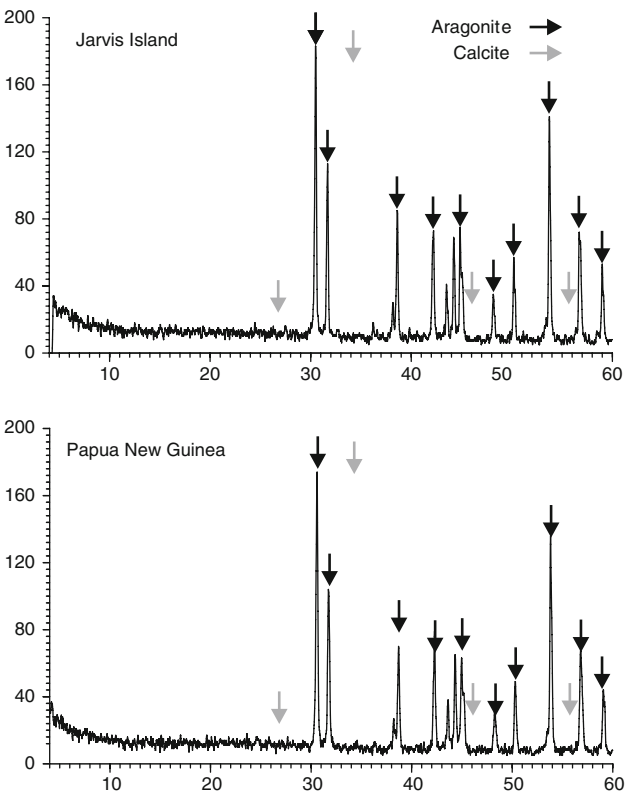

Fig. 1 XRD spectra for both modern (top) and fossil (bottom) *Porites* coral specimens with the standard peaks for aragonite (black arrows) correlating to all peaks in both spectra and standard peaks for calcite (grey arrows) showing no correlation in either spectra, indicating the detection of aragonite only in both samples

2005). The polished slides were carbon coated and silver paint was applied around the edges of each slide to reduce surface charge.

EBSD analyses were performed in a FEI Quanta 200F field emission scanning electron microscope (SEM) equipped with a TSL EBSD system running OIM software version 4. Analyses were carried out in high vacuum mode with a beam aperture of 50 μm and an accelerating voltage of 20 kV. The Kikuchi patterns were indexed using the OIM Data Collection database, which contains structure files of calcite and aragonite. The structure files were tested against calcite and aragonite standard thin sections prepared using the above method of mounting and polishing. In testing the structure files, a confidence index (CI) of >0.5 and pattern fit of <2 over an average of 10-trial spot analyses were required to ensure accuracy of indexing. Hough parameters were set to a minimum peak magnitude of 2, minimum peak distance of 19 and peak symmetry of 0.80 and a binned pattern size of 120. OIM maps were subject to two clean-up algorithm procedures to ensure reliable data were displayed (Mahway 2005). Grain CI standardization was applied with a grain tolerance angle of 5° and minimum grain size of two pixels and neighbour CI correlation of CI 0.2. Further partitioning of data was applied with only grains of CI $\geq$ 0.2, Fit $\leq$ 2.9 and IQ $\geq$ 19 displayed in the resultant OIM map to remove any background noise from the final dataset.

Results and discussion

XRD revealed only aragonite in both the modern and fossil *Porites* coral (Fig. 1). Absence of calcite diffraction suggests that the samples may be pristine and could therefore be considered suitable for climate proxy application.

EBSD analyses clearly define the coral ultrastructure with aragonite fibres in bundles, radiating from the centres of calcification (COC; Fig. 2b, d). The poor diffraction

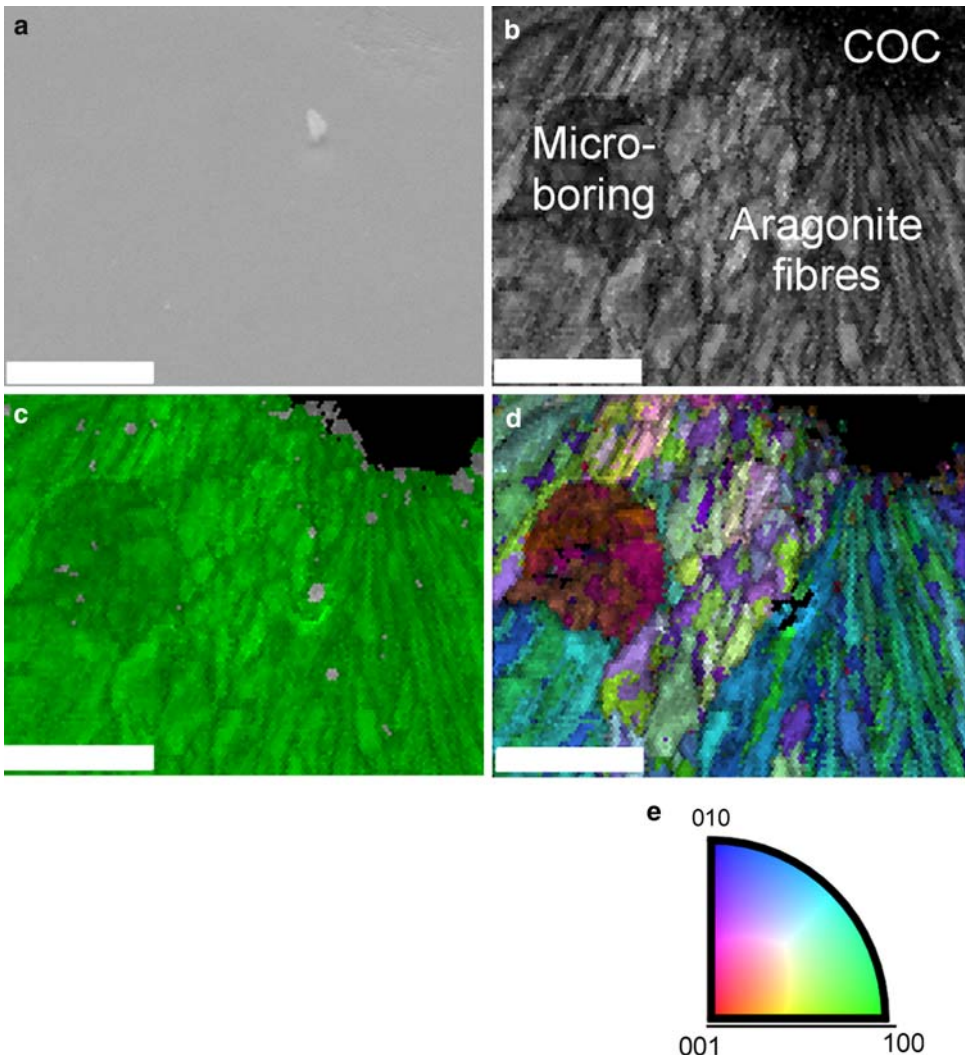

Fig. 2 EBSD analysis of *Porites* coral from Jarvis Island. All four images are of the same area. Scale bar = 10 μm. (**a**) Secondary electron image of polished area of *Porites* coral analysed using EBSD. (**b**) Diffraction intensity map, in which brighter areas are those that have diffracted the electron beam most strongly. Dark area at top right indicates the poor diffraction of the COC. (**c**) Combined diffraction intensity and phase map with green indicating aragonite. (**d**) Map of combined diffraction intensity and crystallographic orientation of the same area (obtained simultaneously), with mainly blue and green colour coding with reference to the key (**e**), indicating that the {010} and {100} planes of aragonite are normal to the plane of view indicating that the {001} is concurrent with the fibre axis. Secondary aragonite cement in the microboring has a different crystallographic orientation to the original aragonite fibres with the 001 plane normal to the plane of view, which is why cement appears red in the image

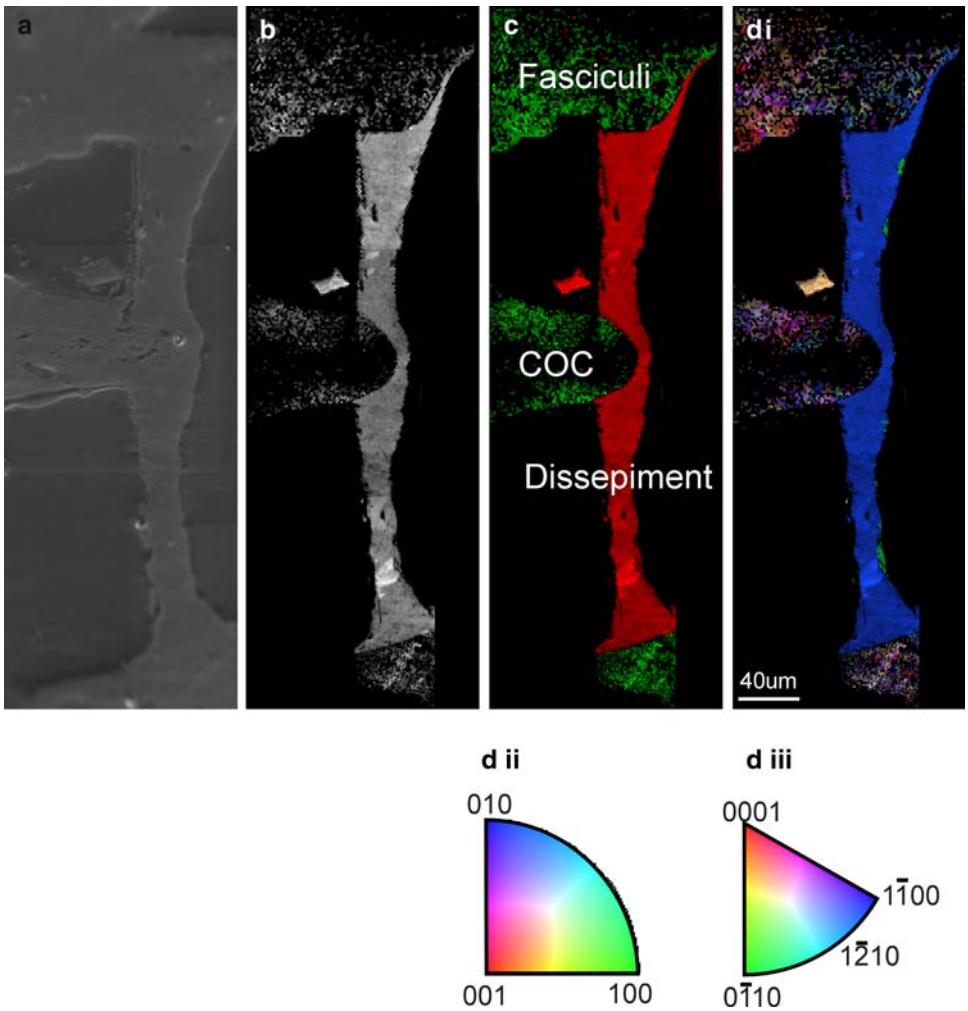

Fig. 3 EBSD maps of an altered dissepiment of fossil *Porites* coral from Papua New Guinea. All four images are of the same area. Scale bar = 40 μm. Individual areas of interest are labelled, centre of calcifications (COC) (**a**), secondary electron image of analysis area, (**b**) diffraction intensity map of area in (**a**). (**c**) Combined diffraction intensity and phase map with calcite shown in red and aragonite in green. (**d i**) Combined diffraction intensity and crystallographic orientation map of calcite and aragonite with crystallographic planes normal to plane of view, coloured according to keys, (**d ii**) for aragonite and (**d iii**) for calcite. Therefore, the uniform colour of the calcite in (**d i**) represents an uniform crystallographic orientation

quality from the COC may be a consequence of a high organic content or nano-scale crystal size as in regions of avian eggshells (Dalbeck and Cusack 2006). The *c*-axis of aragonite is coincident with the fibre length by regular alternation of {010} and {100} faces displayed from neighbouring fibres at the analysis surface. A circular microboring ~10 μm diameter containing aragonite infilling (Fig. 2c, d) is clearly evident in the EBSD analysis of the modern sample (Fig. 2b, d), exhibiting markedly different crystallographic orientation to the surrounding material, with the *c*-axis orientation perpendicular to the analysis surface (Fig. 2d). The boring is not visible in the secondary electron image (Fig. 2a). The phase map indicates that the microboring contains aragonite cement (Fig. 2c).

With corals being used frequently in climate studies, it is essential to ensure that pristine primary aragonite is analysed to provide reliable results. Previous studies have discussed the possibility of other primary mineralised material produced by modern coral (Vandermeule and Watabe 1973; Constantz and Meike 1989; Meibom et al. 2008). No evidence of any material other than aragonite was detected in the modern *Porites* sample using XRD or EBSD. However, some of that aragonite is secondary cement filling microborings (Fig. 2). The presence of secondary aragonite cements precipitated in coral skeletons can affect climate proxies (Quinn and Taylor 2006; Allison et al. 2007; Hendy et al. 2007; Nothdurft et al. 2007), with the secondary aragonite showing chemical variation that can affect the expected climatic record. For example, Allison et al. (2007) showed that 2% secondary aragonite could account for as much as 0.9°C deviation from Sr/Ca estimates of SST.

Although calcite was not detected in XRD analyses of bulk samples of fossil *Porites* specimen here (Fig. 1), EBSD reveals the preferential replacement of the aragonite of the dissepiments by calcite (Fig. 3c, d). The calcite of the dissepiments diffracts the electron beam more intensively than the aragonite of the fasciculi (Fig. 3b). The calcite of the dissepiments occurs in single crystal domains with single orientation, more than 100 μm long as indicated by the crystallographic orientation map (Fig. 3d i). The preferential replacement of aragonite of the

dissepiments is likely to be a consequence of the relatively high surface area of their structure. Alternatively, the horizontal position of the dissepiments may render them more susceptible to alteration.

Diagenetic replacement by another mineral such as calcite may go undetected if the concentration of the secondary mineral is below the threshold of detection by XRD (Fig. 1). Due to the different atomic structures of the two $CaCO_3$ polymorphs, preferential trace element incorporation between the two minerals (Kinsman and Holland 1969; Gaetani and Cohen 2004, 2006b; Mucci et al. 1989; Zhong and Mucci 1989) can produce significant offsets from expected SST estimates, greater than those for secondary aragonite (Allison et al. 2007, Nothdurft et al. 2007).

The results of this study demonstrate that EBSD analysis provides a powerful tool for the investigation of even very early stage coral diagenesis. While XRD remains a valuable means of screening for diagenetic alteration, EBSD has the advantage over XRD and Raman spectroscopy of being able to identify secondary aragonite (Fig. 2c, d). The spatial resolution of EBSD, at the micrometre to nanometre scale, makes it highly suitable for such screening in advance of collecting climate proxy data on a similar spatial scale using techniques such as SIMS, LA-ICP-MS (Fallon et al. 2002) and EPMA. EBSD can therefore complement SIMS analysis (Allison et al. 2007) or Raman spectroscopy (Nothdurft et al. 2007) prior to analysis of environmental proxies. A further advantage of EBSD analysis is that it does not damage the sample area analysed. Thus, EBSD can be used to screen for alteration and then, exactly the same area analysed to obtain climate proxy data from pristine primary aragonite.

Acknowledgements The authors all gratefully acknowledge financial support from the Leverhulme Trust (F/100179/X) and UK Natural Environment Research Council (NER/T/S2002/00443 and GR3/12021). John Gilleece is thanked for his assistance in sample preparation, Peter Chung for valuable assistance in EBSD and SEM analyses and Robert McDonald for assistance with XRD. This work is in keeping with the aims of Theme 3 of the Scottish Alliance for Geoscience, Environment and Society (SAGES).

References

Adams BL, Wright SI, Kunze K (1993) Orientation imaging - the emergence of a new microscopy. Metall Mater Trans A 24: 819–831

Alam MN, Blackman M, Pashley DW (1954) High-angle kikuchi patterns. Proc R Soc Lond A 221:224–242

Allison N, Finch AA (2004) High-resolution Sr/Ca records in modern *Porites lobata* corals: effects of skeletal extension rate and architecture. G-cubed 5:Q05001. doi:05010.01029/02004GC000696

Allison N, Finch AA, Newville M, Sutton SR (2005) Strontium in coral aragonite: 3. Sr coordination and geochemistry in relation to skeletal architecture. Geochim Cosmochim Acta 69:3801–3811

Allison N, Finch AA, Webster JM, Clague DA (2007) Palaeoenvironmental records from fossil corals: the effects of submarine diagenesis on temperature and climate estimates. Geochim Cosmochim Acta 71:4693–4703

Cartwright JHE, Checa AG (2006) The dynamics of nacre self-assembly. J R Soc Interface 4:491–504

Chappell J (1974) Geology of coral terraces, Huon-Peninsula, New-Guinea - study of Quaternary tectonic movements and sea-level changes. Bull Geol Soc Am 85:553–570

Charles CD, Cobb KM, Moore MD, Fairbanks RG (2003) Monsoon-tropical ocean interaction in a network of coral records spanning the 20th century. Mar Geol 201:207–222

Cobb KM, Charles CD, Cheng H, Edwards RL (2003) El Niño southern oscillation and tropical Pacific climate during the last millennium. Nature 424:271–276

Cohen AL, McConnaughey TA (2003) Geochemical perspectives on coral mineralization. In: Dove PM, De Yoreo JJ, Weiner S (eds) Biomineralization. Rev Mineral Geochem 54:151–187

Cohen AL, Owens KE, Layne GD, Shimizu N (2002) The effect of algal symbionts on the accuracy of Sr/Ca paleotemperatures from coral. Science 296:331–333

Cohen AL, Smith SR, McCartney MS, van Etten J (2004) How Brain Corals Record Climate: An Integration of Skeletal Structure, Growth and Chemistry in *Diploria labyrinthiformis* on Bermuda. Mar Ecol Prog Ser 271:147–158

Cole JE (2003) Holocene coral records: windows on tropical climate variability. In: Mackay A, Battarbee R, Birks J, Oldfield F (eds) Global change in the Holocene. Arnold, London, pp 168–184

Constantz BR, Meike A (1989) Calcite centers of calcification in *Mussa angulosa* (Scleractinia). In: Crick RE (ed) Origin, evolution and modern aspects of biomineralization in plants and animals. Plenum Press, New York, pp 201–207

Correge T (2006) Sea surface temperature and salinity reconstruction from coral geochemical tracers. Palaeogeogr Palaeoclimatol Palaeoecol 232:408–428

Cusack M, Pérez-Huerta A, Dalbeck P (2007) Common crystallographic control in calcite biomineralization of bivalved shells. Cryst Eng Comm 9:1215–1218

Cusack M, England J, Parkinson D, Dalbeck P, Lee M, Curry GB, Fallick AE (2008) Oxygen isotope composition, magnesium distribution and crystallography of *Terebratulina retusa*. Fossils & Strata 54:259–267

Dalbeck P, Cusack M (2006) Crystallography (electron backscatter diffraction) and chemistry (electron probe microanalysis) of the avian eggshell. Crystal Growth and Design 6:2558–2562

Dalbeck P, England J, Cusack M, Lee MR, Fallick AE (2006) Crystallography and chemistry of the calcium carbonate polymorph switch in *M. edulis* shells. Eur J Mineral 18:601–609

Dingley DJ (1981) A comparison of diffraction techniques for the SEM. Scanning Electron Microscopy 4:273–286

Dingley DJ (1984) Diffraction from sub-micron areas using electron backscattering in a scanning electron-microscope. Scanning Electron Microscopy 11:569–575

Dingley DJ, Razavizadeh N (1981) The use of Kossel diffraction in the SEM for precision crystallographic studies in metallurgy, mineralogy and semiconductor-materials. Scanning Electron Microscopy 4:287–294

England J, Cusack M, Dalbeck P, Perez-Huerta A (2007) Comparison of the crystallographic structure of semi nacre and nacre by electron backscatter diffraction. Crystal Growth and Design 7:307–310

Esat TM, McCulloch MT, Chappell J, Pillans B, Omura A (1999) Rapid fluctuations in sea level recorded at Huon Peninsula during the penultimate deglaciation. Science 283:197–201

Evans MN, Fairbanks RG, Rubenstone JL (1998) A proxy index of ENSO teleconnections. Nature 394:732–733

Fallon SJ, White JC, McCulloch MT (2002) *Porites* corals as recorders of mining and environmental impacts: Misima Island, Papua New Guinea. Geochim Cosmochim Acta 66:45–62

Felis T, Pätzold J (2003) Climate records from corals. In: Wefer GLF, Mantoura F (eds) Marine science frontiers for Europe. Springer-Verlag, Berlin, pp 11–27

Gabitov RI, Cohen AL, Gaetani GA, Holcomb M, Watson EB (2006) The impact of crystal growth rate on element ratios in aragonite: an experimental approach to understanding vital effects. Geochim Cosmochim Acta 70:A187

Gaetani GA, Cohen AL (2004) Experimental investigation of the partitioning of Mg^{2+}, Ca^{2+}, Sr^{2+}, and Ba^{2+} between aragonite and seawater at 5 to 45°C. Geochim Cosmochim Acta 68:A209

Gaetani GA, Cohen AL (2006a) Calculating paleotemperatures from the elemental composition of coral skeleton: a new approach to old proxies. Geochim Cosmochim Acta 70:A187

Gaetani GA, Cohen AL (2006b) Element partitioning during precipitation of aragonite from seawater: a framework for understanding paleoproxies. Geochim Cosmochim Acta 70:4617–4634

Gagan MK, Ayliffe LK, Beck JW, Cole JE, Druffel ERM, Dunbar RB, Schrag DP (2000) New views of tropical paleoclimates from corals. Quaternary Sci Rev 19:4564

Grottoli AG, Eakin M (2007) A review of coral δ18O and Δ14C proxy records. Earth Sci Rev 81:67–91

Guilderson TP, Fairbanks RG, Rubenstone JL (1994) Tropical temperature variations since 20,000 years ago - modulating interhemispheric climate-change. Science 263:663–665

Guilderson TP, Fairbanks RG, Rubenstone JL (2001) Tropical Atlantic coral oxygen isotopes: glacial–interglacial sea surface temperatures and climate change. Mar Geol 172:75–89

Hendy EJ, Gagan MK, Lough JM, McCulloch M, deMenocal PB (2007) Impact of skeletal dissolution and secondary aragonite on trace element and isotopic climate proxies in *Porites* corals. Paleoceanography 22:PA4101. doi:4110.1029/2007PA001462

Hughen KA, Schrag DP, Jacobsen SB, Hantoro W (1999) El Nino during the last interglacial period recorded by a fossil coral from Indonesia. Geophys Res Lett 26:3129–3132

Jenkins R, Snyder RL (1996) Introduction to X-ray powder diffractometry. Wiley, New York

Kinsman DJJ, Holland HD (1969) Co-precipitation of cations with $CaCO_3$ IV. Co-precipitation of Sr^{2+} with aragonite between 16 and 96°C. Geochim Cosmochim Acta 33:1–18

Kuhnert H, Crüger T, Pätzold J (2005) NAO signature in a Bermuda coral Sr/Ca record, G-cubed 6:Q04004. doi:10.1029/2004GC000786

Mahway E (2005) OIM user's manual. EDAX-TSL, New Jersey

Maier C, Felis T, Patzold J, Bak RPM (2004) Effect of skeletal growth and lack of species effects in the skeletal oxygen isotope climate signal within the coral genus *Porites*. Mar Geol 207:193–208

Marriott CS, Henderson GM, Crompton R, Staubwasser M, Shaw S (2004) Effect of mineralogy, salinity, and temperature on Li/Ca and Li isotope composition of calcium carbonate. Chem Geol 212:5–15

Meibom A, Stage M, Wooden J, Constantz BR, Dunbar RB, Owen A, Grumet N, Bacon CR, Chamberlain CP (2003) Monthly strontium/calcium oscillations in symbiotic coral aragonite: biological effects limiting the precision of the paleotemperature proxy. Geophys Res Lett 30. doi:10.1029/2002GL016864

Meibom A, Cuif JP, Hillion FO, Constantz BR, Juillet-Leclerc A, Dauphin Y, Watanabe T, Dunbar RB (2004) Distribution of magnesium in coral skeleton. Geophys Res Lett 31:L23306. doi:23310.21029/22004GL021313

Meibom A, Yurimoto H, Cuif JP, Domart-Coulon I, Houlbreque F, Constantz B, Dauphin Y, Tambutte E, Tambutte S, Allemand D, Wooden J, Dunbar R (2006) Vital effects in coral skeletal composition display strict three-dimensional control. Geophys Res Lett 33:L11608. doi:10.1029/2006GL025968

Meibom A, Mostefaoui S, Cuif JP, Dauphin Y, Houlbreque F, Dunbar R, Constantz B (2007) Biological forcing controls the chemistry of reef-building coral skeleton. Geophys Res Lett 34:L02601. doi:10.1029/2006GL028657

Meibom A, Cuif J-P, Houlbreque F, Mostefaoui S, Dauphin Y, Meibom KL, Dunbar R (2008) Compositional variations at ultra-structure length-scales in coral skeleton. Geochim Cosmochim Acta 72:1555–1569

Mitsuguchi T, Matsumoto E, Uchida T (2003) Mg/Ca and Sr/Ca ratios of *Porites* coral skeleton: evaluation of the effect of skeletal growth rate. Coral Reefs 22:381–388

Mucci A, Canuel R, Zhong SJ (1989) The solubility of calcite and aragonite in sulfate-free seawater and the seeded growth-kinetics and composition of the precipitates at 25°C. Chem Geol 74:309–320

Muller A, Gagan MK, McCulloch MT (2001) Early marine diagenesis in corals and geochemical consequences for paleoceanographic reconstructions. Geophys Res Lett 28:4471–4474

Nishikawa S, Kikuchi S (1928a) Diffraction of cathode rays by mica. Nature 121:1019–1020

Nishikawa S, Kikuchi S (1928b) Diffraction of cathode rays by calcite. Nature 122:726–726

Nothdurft LD, Webb GE, Bostrom T, Rintoul L (2007) Calcite-filled borings in the most recently deposited skeleton in live-collected Porites (Scleractinia): implications for trace element archives. Geochim Cosmochim Acta 71:5423–5438

Nowell MM, Witt RA, True B (2005) EBSD sample preparation: techniques tips and tricks. Micros Microanal 11:504–505

Perez-Huerta A, Cusack M, England J (2007) Crystallography and diagenesis in fossil craniid brachiopods. Palaeontology 50: 757–763

Prior DJ, Boyle AP, Brenker F, Cheadle MC, Day A, Lopez G, Peruzzo L, Potts GJ, Reddy S, Spiess R, Timms NE, Trimby P, Wheeler J, Zetterstrom L (1999) The application of electron backscatter diffraction and orientation contrast imaging in the SEM to textural problems in rocks. Am Mineral 84:1741–1759

Quinn TM, Taylor FW (2006) SST artifacts in coral proxy records produced by early marine diagenesis in a modern coral from Rabaul, Papua New Guinea. Geophys Res Lett 33:L04601. doi:10.1029/2005GL024972

Schmahl WW, Griesshaber E, Neuser R, Lenze A, Job R, Brand U (2004) The microstructure of the fibrous layer of terebratulide brachiopod shell calcite. Eur J Mineral 16:693–697

Schwartz AJ (2000) Electron backscatter diffraction in materials science. Plenum Press, New York

Schwarzer RA (1997a) Advances in crystal orientation mapping with the SEM and TEM. Ultramicroscopy 67:19–24

Schwarzer RA (1997b) Automated crystal lattice orientation mapping using a computer-controlled SEM. Micron 28:249–265

Tudhope AW, Shimmield GB, Chilcott CP, Jebb M, Fallick AE, Dalgleish AN (1995) Recent changes in climate in the far western equatorial Pacific and their relationship to the southern oscillation; oxygen isotope records from massive corals, Papua New Guinea. Earth Planet Sci Lett 136:575–590

Tudhope AW, Lea DW, Shimmield GB, Chilcott CP, Head S (1996) Monsoon climate and Arabian Sea coastal upwelling recorded in massive corals from southern Oman. Palaios 11:347–361

Tudhope AW, Chilcott CP, McCulloch MT, Cook ER, Chappell J, Ellam RM, Lea DW, Lough JM, Shimmield GB (2001) Variability in the El Niño - Southern oscillation through a glacial-interglacial cycle. Science 291:1511–1517

Urban FE, Cole JE, Overpeck JT (2000) Influence of mean climate change on climate variability from a 155-year tropical Pacific coral record. Nature 407:989–993

Vandermeule JH, Watabe N (1973) Studies on reef corals.1. Skeleton formation by newly settled planula larva of Pocillopora-damicornis. Mar Biol 23:47–57

Venables JA, Harland CJ (1973) Electron backscattering patterns - new technique for obtaining crystallographic information in scanning electron-microscope. Phil Mag A 27:1193–1200

Wilson RA, Tudhope AW, Brohan P, Briffa KR, Osborn TJ, Tett SBF (2006) 250-years of reconstructed and modeled tropical temperatures. J Geophys Res 111:C10007. doi:10010.11029/12005JC003188

Woodroffe CD, Gagan MK (2000) Coral microatolls from the central Pacific record late Holocene El Niño. Geophys Res Lett 27: 1511–1514

Wright SI, Adams BL (1991) Automated lattice orientation determination from electron backscatter kikuchi diffraction patterns. Texture Microstruct 14:273–278

Wright SI, Adams BL (1992) Automatic-analysis of electron backscatter diffraction patterns. Metall Mater Trans A 23:759–767

Wright SI, Gray GT, Rollett AD (1994) Textural and microstructural gradient effects on the mechanical-behavior of a Tantalum plate. Metall Mater Trans A 25:1025–1031

Zhong SJ, Mucci A (1989) Calcite and aragonite precipitation from seawater solutions of various salinites - precipitation rates and overgrowth compositions. Chem Geol 78:283–299